SIMULTANEOUS ROBUST FITTING OF MULTIPLE CURVES

Jean-Philippe Tarel
ESE, Laboratoire Central des Ponts et Chaussées, 58 Bd Lefebvre, 75015 Paris, France
Tarel@lcpc.fr

Pierre Charbonnier
ERA 27 LCPC, Laboratoire des Ponts et Chaussées, 11 rue Jean Mentelin, B.P. 9, 67035 Strasbourg, France
Pierre.Charbonnier@equipement.gouv.fr

Sio-Song Ieng
ERA 17 LCPC, Laboratoire des Ponts et Chaussées, 23 avenue de l'amiral Chauvin, B.P. 69, 49136 Les Ponts de Cé, France
Sio-Song.Ieng@equipement.gouv.fr

Keywords: Image Analysis, Statistical Approach, Robust Fitting, Multiple Fitting, Image Grouping and Segmentation.

Abstract: In this paper, we address the problem of robustly recovering several instances of a curve model from a single noisy data set with outliers. Using M-estimators revisited in a Lagrangian formalism, we derive an algorithm that we call SMRF, which extends the classical Iterative Reweighted Least Squares algorithm (IRLS). Compared to the IRLS, it features an extra probability ratio, which is classical in clustering algorithms, in the expression of the weights. Potential numerical issues are tackled by banning zero probabilities in the computation of the weights and by introducing a Gaussian prior on curves coefficients. Applications to camera calibration and lane-markings tracking show the effectiveness of the SMRF algorithm, which outperforms classical Gaussian mixture model algorithms in the presence of outliers.

1 INTRODUCTION

In this paper, we propose a method for robustly recovering several instances of a curve model from a single noisy data set with severe perturbations (outliers). It is based on an extension of the work reported in (Tarel et al., 2002), in which M-estimators are revisited in an Lagrangian formalism which leads to a new derivation and convergence proof of the well-known Iterative Reweighted Least Squares (IRLS) algorithm. Following the same approach based on the Lagrangian framework, we derive, in a natural way, a deterministic, alternate minimization algorithm, for Simultaneous Multiple Robust Fitting (SMRF) which extends the IRLS algorithm. Compared to the IRLS, the SMRF features an extra probability ratio, which is classical in clustering algorithms, in the expression of the weights. Potential numerical issues are tackled by banning zero probabilities in the computation of the weights and by introducing a Gaussian prior on the curves coefficients. Such a prior is, moreover, well-suited to sequential image processing and provides control on the curves. Applications to camera calibration and lane-markings tracking illustrate the effectiveness of the SMRF algorithm. In particular, it outperforms classical Gaussian mixture model algorithms in the presence of outliers.

The paper is organized as follows. In Sec. 2, we present the robust multiple curves estimation problem and introduce our algorithmic strategy. The resulting algorithm is given in Sec. 3. Technical details on its derivation and convergence proof are given in the Appendix. In Sec. 4, connections are made with other approaches in the domain. Finally, we apply the algorithm to road tracking and to camera calibration, in Sec. 5.

2 MULTIPLE ROBUST MAXIMUM LIKELIHOOD ESTIMATION (MLE)

In this section, we model the problem of simultaneously fitting m curves in a robust way. Each individual curve is explicitly described by a vector parameter $\tilde{A}_j$, $1 \leq j \leq m$. The observations, y, are given by a linear generative model:

$$y = X(x)^t \tilde{A}_j + b \tag{1}$$

where (x,y) are the image coordinates of a data point, $\tilde{A}_j = (\tilde{a}_{ij})_{0 \leq i \leq d}$ is the vector of curve parameters and

$X(x) = (f_i(x))_{0 \leq i \leq d}$ is the vector of basis functions at the image coordinate x, which will be denoted as X for the sake of simplicity. These vectors are of size $d+1$. Example of basis functions will be given in Sec. 5.2. Note that we consider the *fixed design* case, i.e. in (1), x is assumed non-random. In that case, it is shown that certain M-estimators attain the maximum possible breakdown point of approximately 50% (Mizera and Müller, 1999). In all that follows, the measurement noise b is assumed independent and identically distributed (iid) and centered. In order to render the estimates robust to non-Gaussian noise (outliers), we formulate the noise distribution as:

$$p_s(b) \propto \frac{1}{s} e^{-\frac{1}{2}\phi((\frac{b}{s})^2)} \tag{2}$$

where $\propto$ denotes the equality up to a factor, and s is the scale of the pdf. As stated in (Huber, 1981), the role of ϕ is to saturate the error in case of a large noise $|b| = |X^t \tilde{A}_j - y|$, and thus to lower the importance of outliers. The scale parameter, s, controls the distance from which noisy measurements have a good chance of being considered as outliers. As in the half-quadratic approach (Geman and Reynolds, 1992; Charbonnier et al., 1997; Tarel et al., 2002), $\phi(t)$ must fulfill the following hypotheses:

- **H0**: defined and continuous on $[0, +\infty[$ as well as its first and second derivatives,
- **H1**: $\phi'(t) > 0$ (thus ϕ is increasing),
- **H2**: $\phi''(t) < 0$ (thus ϕ is concave).

Note that these assumptions are very different from those used in (Huber, 1981), where the convergence proof required that the potential function $\rho(b) = \phi(b^2)$ be convex. In the present case, the concavity and monotonicity requirements imply that $\phi'(t)$ is bounded, but $\phi(b^2)$ is not *necessarily convex* w.r.t. b.

Our goal is to simultaneously estimate the m curve parameter vectors $A_{j=1,\cdots,m}$ from the whole set of n data points (x_i, y_i), $i = 1, \cdots, n$. The probability of a measurement point (x_i, y_i), given the m curves is the sum of the probabilities over each curve:

$$p_i((x_i,y_i)|A_{j=1,\cdots,m}) \propto \frac{1}{s} \sum_{j=1}^{j=m} e^{-\frac{1}{2}\phi((\frac{X_i^t A_j - y_i}{s})^2)}.$$

Concatening all curve parameters into a single vector $A = (A_j), j = 1, \cdots, m$ of size $m(d+1)$, we can write the probability of the whole set of points as the product of the individual probabilities:

$$p((x_i,y_i)_{i=1,\cdots,n}|A) \propto \frac{1}{s^n} \prod_{i=1}^{i=n} \sum_{j=1}^{j=m} e^{-\frac{1}{2}\phi((\frac{X_i^t A_j - y_i}{s})^2)} \tag{3}$$

Maximizing the likelihood $p((x_i,y_i)_{i=1,\cdots,n}|A)$ is equivalent to minimizing the negative of its logarithm:

$$e_{MLE}(A) = \sum_{i=1}^{i=n} -\ln(\sum_{j=1}^{j=m} e^{-\frac{1}{2}\phi((\frac{X_i^t A_j - y_i}{s})^2)}) + n\ln(s) \tag{4}$$

Using the same trick as the one described in (Tarel et al., 2002) for robust fitting of a single curve, we introduce the auxiliary variables $w_{ij} = (\frac{X_i^t A_j - y_i}{s})^2$, as explained in the Appendix. We then rewrite the value $e_{MLE}(A)$ as the value achieved at the unique saddle point of the following Lagrange function:

$$\begin{aligned} L_R &= \sum_{i=1}^{i=n} \sum_{j=1}^{j=m} \frac{1}{2} \lambda_{ij} (w_{ij} - (\frac{X_i^t A_j - y_i}{s})^2) \\ &+ \sum_{i=1}^{i=n} \ln(\sum_{j=1}^{j=m} e^{-\frac{1}{2}\phi(w_{ij})}) - n\ln(s) \end{aligned} \tag{5}$$

Then, the algorithm obtained by alternated minimizations of the dual function w.r.t. λ_{ij} and A is globally convergent, towards a local minimum of $e_{MLE}(A)$, as shown in the Appendix.

3 SIMULTANEOUS MULTIPLE ROBUST FITTING ALGORITHM

As detailed in the Appendix, minimizing (5) leads to alternate between the three sets of equations:

$$w_{ij} = (\frac{X_i^t A_j - y_i}{s})^2, 1 \leq i \leq n, 1 \leq j \leq m, \tag{6}$$

$$\lambda_{ij} = \frac{e^{-\frac{1}{2}\phi(w_{ij})}}{\sum_{k=1}^{k=m} e^{-\frac{1}{2}\phi(w_{ik})}} \phi'(w_{ij}), 1 \leq i \leq n, 1 \leq j \leq m, \tag{7}$$

$$(\sum_{i=1}^{i=n} \lambda_{ij} X_i X_i^t) A_j = \sum_{i=1}^{i=n} \lambda_{ij} y_i X_i, 1 \leq j \leq m \tag{8}$$

In practice, some care must be taken, to avoid numerical problems and singularities. First, it is important that the denominator in (7) be numerically non-zero, which might occur for a data point located far from all curves. Zero probabilities are banned by adding a small value ε (equal to the machine precision) to the exponential in the probability p_i of a measurement point. As a consequence, when a point with index i is far from all curves, $\phi'(w_{ij})$ is weighted by a constant factor, $1/m$, in (7).

Second, the linear system in (8) can be singular. To avoid this, it is necessary to enforce a Gaussian prior on the whole curves parameters with bias A^{pr}

and covariance matrix C^{pr}. Note that the reason for introducing such a prior is not purely technical: it is indeed a very simple and useful way of taking into account application-specific a priori knowledge, as shown in Sec. 5.3 and 5.4. A default prior can be used. In practice, we found very useful the following default prior: the bias is zero, i.e $A^{pr} = 0$, and the inverse covariance matrix is block diagonal where each diagonal block equals:

$$C^{pr-1} = r \int_{-1}^{1} X(x)X(x)^t dx \qquad (9)$$

assuming that $[-1,1]$ is the range where x varies. The regularization term $(A-A^{pr})^t C^{pr-1}(A-A^{pr})$ is added to (4) and (5). Therefore, the parameter r allows us to balance between the data fidelity term and the prior. The advantage of the default prior described above is that it is a model of the perturbations due to the image sampling.

Finally, the Simultaneous Multiple Robust Fitting algorithm (SMRF) is:

1. Initialize the number of curves m, the vector $A^0 = (A^0_j)$, $1 \leq j \leq m$, which gathers all curves parameters and set the iteration index to $k = 1$.
2. For all indexes i, $1 \leq i \leq n$, and j, $1 \leq j \leq m$, compute the auxiliary variables $w^k_{ij} = (\frac{X_i^t A_j^{k-1} - y_i}{s})^2$ and the weights $\lambda^k_{ij} = \frac{\varepsilon + e^{-\frac{1}{2}\phi(w^k_{ij})}}{m\varepsilon + \sum_{j=1}^{j=m} e^{-\frac{1}{2}\phi(w^k_{ij})}} \phi'(w^k_{ij})$.
3. Solve the linear system:

$$\left[D + C^{pr-1}\right] A^k = \begin{bmatrix} \sum_{i=1}^{i=n} \lambda^k_{i1} y_i X_i \\ \vdots \\ \sum_{i=1}^{i=n} \lambda^k_{im} y_i X_i \end{bmatrix} + C^{pr-1} A^{pr}.$$

4. If $\|A^k - A^{k-1}\| > \varepsilon'$, increment k, and go to 2, else the solution is $A = A^k$.

In the above algorithm, D is the block-diagonal matrix whose m diagonal blocks are the matrices $\sum_{i=1}^{i=n} \lambda^k_{ij} X_i X_i^t$ of size $(d+1)\times(d+1)$, with $1 \leq j \leq m$. The prior covariance matrix C^{pr} is of size $m(d+1)\times m(d+1)$. The prior bias A^{pr} is a vector of size $m(d+1)$, as well as A and A^k. The complexity is $O(nm)$ for the step 2, and $O(m^2(d+1)^2)$ for the step 3 of the algorithm.

4 CONNECTIONS WITH OTHER APPROACHES

The proposed algorithm has important connections with previous works in the field of regression and clustering and we would like to highlight a few of them.

In the single curve case, $m = 1$, the SMRF algorithm is reduced to the so-called Iterative Reweighted Least Squares extensively used in M-estimators (Huber, 1981) and half-quadratic theory (Charbonnier et al., 1997; Geman and Reynolds, 1992). The SMRF and IRLS algorithms share very similar structures and it is important to notice that the main difference is within the Lagrange multipliers λ_{ij}, see (7). Compared to the IRLS, the λ_{ij} are just weighted by an extra probability ratio, which is classical in clustering algorithms.

To make the connection with clustering clearer, let us substitute $Y = A_j + b$ to the generative model (1), where Y and A_j are vectors of same size and respectively denote a data points and a cluster centroid. The derivation described in Sec. 3 is still valid and the obtained algorithm turns to be a clustering algorithm with m clusters, each cluster being represented by a vector, its centroid. The probability distribution of a cluster around its centroid is directly specified by the function ϕ. The obtained algorithm is thus able of modeling the Y_i's by a mixture of pdfs which are not necessarily Gaussian. The mixture problem is usually solved by the well-known Expectation-Minimization (EM) approach (Dempster et al., 1977). In the non-Gaussian case, the minimization (M) step implements robust estimation, which is an iterative process in itself. Hence, the resulting EM algorithm involves two nested loops, while the proposed algorithm features only one. An alternative to the EM approach is the Generalized EM (GEM) approach which consists in performing an approximate M-step: typically, only one iteration rather than the full minimization. The resulting algorithm in the robust case is identical to the one we derived in the Lagrangian framework (apart from the regularization of the singular cases). In our formalism however, no approximation is made in the derivation of the algorithm, in contrast with the GEM approach.

We also found that the SMRF algorithm is very close to an earlier work in the context of clustering (Cambell, 1984). However, to our knowledge, the latter was just introduced as an extra ad-hoc weighting over M-estimators without statistical interpretation and, moreover, singular configurations were not dealt with.

The SMRF algorithm is subject to the initialization problem since it only converges towards a local minimum. To tackle this problem, the Graduated Non Convexity approach (GNC) (Blake and Zisserman, 1987) is used to improve the chances of converging towards the global minimum. Details are given

in Sec. 5.4. The SMRF can be also used as a fitting process within the RANSAC (Hartley and Zisserman, 2004) approach to improve the convergence towards the global minimum.

5 EXPERIMENTAL RESULTS

The proposed approach being based on a linear generative model, many applications could potentially be addressed using the SMRF algorithm. In this paper, we focus on two specific applications, namely simultaneous lane-markings tracking and camera calibration from a regular lattice of lines with geometric distortions.

5.1 Noise Model

Among the suitable functions for robust estimation, we use a simple parametric family of probability distribution functions, that was introduced in (Tarel et al., 2002) under the name of *smooth exponential family* (SEF), $S_{\alpha,s}$:

$$S_{\alpha,s}(b) \propto \frac{1}{s} e^{-\frac{1}{2}\phi_\alpha((\frac{b}{s})^2)} \qquad (10)$$

where, with $t = (\frac{b}{s})^2$, $\phi_\alpha(t) = \frac{1}{\alpha}((1+t)^\alpha - 1)$.

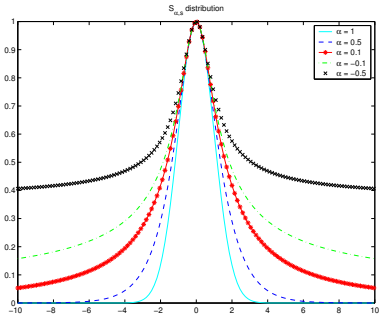

Figure 1: Noise models in the SEF $S_{\alpha,s}$. Notice how the tails become heavier as α decreases.

These laws are shown in Figure 1 for different values of α. The smaller the value of α, the higher the probability of observing large, not to say very large, errors (outliers). This parameter allows a continuous transition between well-known statistical laws such as Gauss ($\alpha = 1$), smooth Laplace ($\alpha = \frac{1}{2}$) and T-Student ($\alpha \to 0$). This can be exploited to get better convergence of the SMRF algorithm by using the GNC approach, i.e. by progressively decreasing α towards 0.

5.2 Road Shape Model

The road shape features (x,y) are given by the lane-marking centers extracted using the local feature extractor described in (Ieng et al., 2004). An example of extraction is shown in Figure 6(b). In practice, we model road lane markings by polynomials $y = \sum_{i=0}^{d} a_i x^i$. Moreover, in the *flat world* approximation, the image of a polynomial on the road under perspective projection is a *hyperbolic polynomial* with equation $y = c_0 x + c_1 + \sum_{i=2}^{d} \frac{c_i}{(x-x_h)^i}$, where c_i is linearly related to a_i. Therefore, the hyperbolic polynomial model is well suited to the case of road scene analysis. To avoid numerical problems, a whitening of the data is performed by scaling the image in a $[-1,1]\times[-1,1]$ box for polynomial curves and in a $[0,1]\times[-1,1]$ box for hyperbolic polynomials, prior to the fitting.

5.3 Geometric Priors

As noticed in Sec. 3, the use of a Gaussian prior allows introducing useful application-specific knowledge. For example, using (9) for the diagonal blocks of the inverse prior covariance matrix, we take into account perturbations due to image sampling.

Tuning the diagonal elements of C^{pr} provides control on the curve degree. For polynomials, the diagonal components of the covariance matrix correspond to monomials of different degrees. The components of degree higher than one are thus set to smaller values than those of degree zero and one.

Geometric smooth constraints between curves can be enforced by using also non-zero off-diagonal blocks, in particular it is a way of maintaining parallelism between curves. As an illustration, to smoothly enforce parallelism between two lines $y = a_0 + a_1 x$ and $y = a'_0 + a'_1 x$, the prior covariance matrix is obtained by rewriting $(a_1 - a'_1)^2$ in matrix notations:

$$\begin{bmatrix} a_0 \\ a_1 \\ a'_0 \\ a'_1 \end{bmatrix}^t \begin{bmatrix} 0 & 0 & 0 & 0 \\ 0 & 1 & 0 & -1 \\ 0 & 0 & 0 & 0 \\ 0 & -1 & 0 & 1 \end{bmatrix} \begin{bmatrix} a_0 \\ a_1 \\ a'_0 \\ a'_1 \end{bmatrix}$$

The above matrix, multiplied by an overall factor can be used as an inverse prior covariance C^{pr-1}. The factor controls the balance between the data fidelity term and the other priors. Other kinds of geometric smooth constraints can be handled in a similar way, such as intersection at a given point, or symmetric orientations. These geometric priors can be combined by adding the associated regularization term $(A - A^{pr})^t C^{pr-1}(A - A^{pr})$ to (4) and (5).

5.4 Lane-Markings Tracking

We shall now describe the application of the SMRF algorithm to the problem of tracking lane markings.

In addition to the previous section, another interesting feature of using a Gaussian prior is that the SMRF is naturally suitable for being included in a Kalman filtering. However, this raises the question of the definition of the posterior covariance matrix of the estimate. Under the Gaussian noise assumption, the estimate of the posterior covariance matrix is well-known for each curve: $C_j = s^2 \left(\sum_{i=1}^{i=n} X_i X_i^t\right)^{-1}$. Unfortunately, in the context of robust estimation, the estimation of C_j for each curve A_j is a difficult issue and only approximate matrices are available. In (Ieng et al., 2004), several approximates were compared. The underlying assumption for defining all these approximates is that the noise is independent. However, we found out that in practice, the noise is correlated from one image line to another. Therefore, all these approximates can be improved by introducing an had-hoc correction factor which accounts for data noise correlations in the inverse covariance matrix. We found experimentally that the following factor is appropriate, for each curve j:

$$1 - \frac{\sum_{i=1}^{i=n-1} \sqrt{\lambda_{ij} w_{ij} \lambda_{i+1,j} w_{i+1,j}}}{\sum_{i=1}^{i=n} \lambda_{ij} w_{ij}}$$

The approximate posterior covariance matrix for the whole set of curve parameters, A, is simply built as a block-diagonal matrix made of the individual posterior covariance matrices for each curve, C_j. This temporal prior can be easily combined with geometric priors to allow tracking of parallel curves for instance.

Figure 2: Detected lane-markings (in green) and uncertainty about curve position (in red).

Figure 2 shows the three curves simultaneously fitted on the lane-marking centers (in green) and the associated uncertainty curves of the horizontal position of each fitted curve ($\pm\sqrt{X(x)^t C_j^{-1} X(x)}$, in red). Notice that the uncertainty on the right sparse lane-marking is higher than for the continuous one on the center. Moreover, the higher the distance to the camera, the higher the uncertainty, since the curve gets closer to possible outliers. In all these experiments, and following, the parameters used for the noise model are $\alpha = 0.1$ and $s = 4$.

(a)

(b)

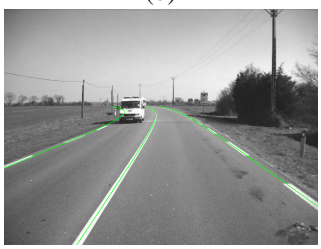

(c)

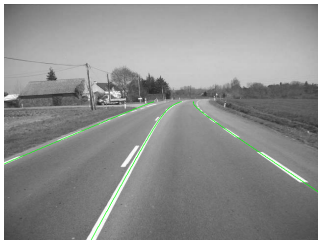

(d)

Figure 3: Two images extracted from a sequence of 240 images processed with, on (a)(b), separate Kalman filters and, on (c)(d), simultaneous Kalman filter. The three detected lane-markings of degree two are in green.

For the tracking itself, we experimented both separate Kalman filters on individual curves, and a simultaneous Kalman filter. The former can be seen as a particular case of the latter, in which the inverse prior covariance matrix C^{pr} is block-diagonal so the linear system of size $m(d+1)$ in the SMRF algorithm can be decomposed as m linear independent systems of size $d+1$. Figure 3 compares the results obtained with separate and simultaneous Kalman filters. No-

tice how the parallelism between curves is better preserved within the simultaneous Kalman filter, thanks to an adequate choice of the off-diagonal blocks of C^{pr}.

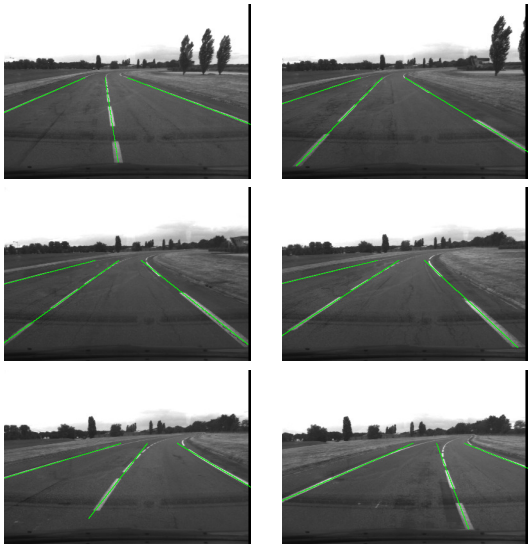

Figure 4: Six of a 150-image sequence, featuring lane changes. Green lines show the three fitted lane-markings centers.

Figure 4 illustrates the ability of the SMRF-based Kalman filter to fit and track several curves in an image sequence. In that case, three lane-markings are simultaneously fitted and correctly tracked, even though the vehicle performs several lane changes during the 150-image sequence. Notice that, while Kalman filtering can incorporate a dynamic model of the vehicle, we only used a static model in these experiments, since only the images were available. We observed that it is better to initialize the SMRF algorithm with the parameters resulting from the fitting on the previous image, rather than with the filtered parameters: filtering indeed introduces a delay in the case of fast displacements or variations of the tracked curves.

Moreover, we obtained interesting results on difficult road sequences. For instance, Figure 5 shows a short sequence of poor quality images, due to rain. The left lane-marking is mostly hidden on two consecutive images. Thanks to the simultaneous Kalman filter, the SMRF algorithm is able to interpolate correctly the hidden lane-marking.

5.5 Camera Calibration

We now present another application of the SMRF algorithm, in the context of camera calibration. The goal is to estimate accurately the position and orientation of the camera with respect to the road and its intrinsic parameters. A calibration setup made of two sets of perpendicular lines painted on the road is thus observed by a camera mounted on a vehicle, as shown in Figure 6(a). The SMRF algorithm can be used to provide accurate data to the calibration algorithm by estimating the grid intersections. Even though the markings are clearly visible in the image, some of them are quite short, and there are outliers due to the presence of water puddles. Figure 6(b) shows the extracted lane-marking centers. When a Gaussian mixture model is used, the obtained fit is severely troubled by the outliers, as displayed in Figure 6(d), even though the curves are initialized very close to the expected solution, see Figure 6(c).

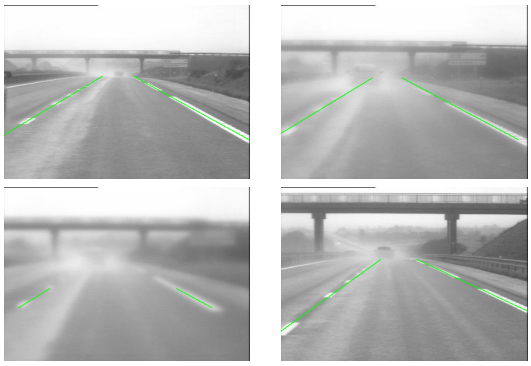

Figure 5: Fitting in adverse conditions: in this excerpt, the left lane-marking is mostly hidden on two successive images.

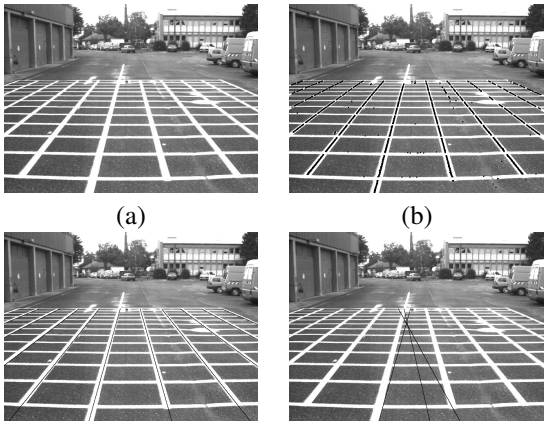

Figure 6: (a) Original image of the calibration grid. (b) Extracted lane-marking centers (outliers are due to puddles). (c) 10 initial lines for the fitting on the vertical markings. (d) Fitted lines on the vertical markings under Gaussian noise assumption.

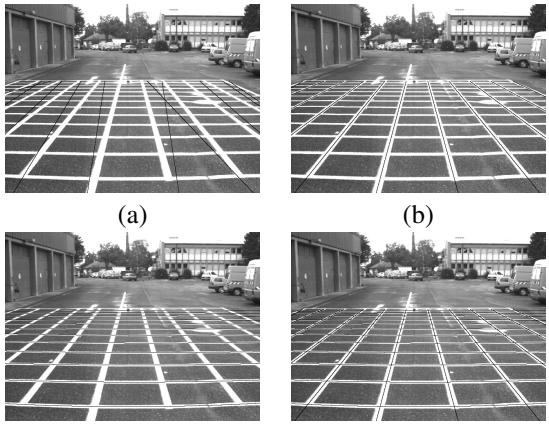

Figure 7: (a) 12 initial lines for the fitting on the vertical markings. (b) The fitting yields 11 different lines. (c) 12 second degree polynomials fitted on the horizontal markings. (d) Results of the horizontal and vertical fitting superimposed.

On the contrary, with the same extracted lane-marking centers, the SMRF algorithm, with noise model parameters $\alpha = 0.1$ and $s = 4$, leads to nice results, as shown in Figure 7(b) for the vertical lines, and in Figure 7(c) for the horizontal curves. 11 different lines were obtained for the vertical markings, and 12 different second degree polynomials were obtained for the horizontal markings. Figure 7(d) shows the two sets of curves superimposed.

We also use these calibration images to investigate the issue of initialization. We typically take a number of curve prototypes higher than the real number of curves in the image, see e.g. Figure 7(a). We observed that the extra prototypes may be either fitted on outliers groups or identical to another fitted prototype (e.g. in Figure 7(b), two resulting curves are identical). Detecting identical curves is easy, for instance by performing a Bayesian recognition test on every pair (A_j, A_k), i.e. comparing $(A_j - A_k)^t C_j^{-1} (A_j - A_k)$ to a small threshold, where C_j is the posterior covariance matrix of the curve A_j. To detect prototypes fitted to only a few points such as outliers, we exploit the uncertainty measure provided by the posterior covariance matrix and simply threshold $-log(det(C_j))$. Finally, notice that the SMRF algorithm does not require to be initialized very close to the expected solution, as illustrated by Figure 7(a)(b).

6 CONCLUSION

In the continuing quest for achieving robustness in detection and tracking curves in images, this paper makes two contributions. The first one is the derivation, in a MLE approach and using Kuhn and Tucker's classical theorem, of the so-called SMRF algorithm. This algorithm extends mixture model algorithm, such as the one derived using EM, to robust curve fitting. It is also an extended version of the IRLS, in which the weights incorporate an extra probability ratio. The second contribution is the regularization of the SMRF algorithm by introducing Gaussian priors on curve parameters and the handling of potential numerical issues by banning zero probabilities in the computation of weights. From our experiments, banning zero probabilities seems to have important positive consequences in pushing the curves to spread out all the data, and thus in providing improved robustness to the initialization, as shown in the context of camera calibration. The introduction of the Gaussian prior is also beneficial in particular in the context of image sequence processing, as illustrated with an application of simultaneous lane-markings tracking on-board a vehicle in adverse conditions. The approach being based on a linear generative model, it is quite generic and we believe that it can be used with benefits in many other fields, such as clustering or appearance modeling.

REFERENCES

Blake, A. and Zisserman, A. (1987). *Visual Reconstruction*. MIT Press, Cambridge, MA.

Boyd, S. and Vandenberghe, L. (2004). *Convex Optimization*. Cambridge University Press.

Cambell, N. A. (1984). Mixture models and atypycal values. *Mathematical Geology*, 16(5):465–477.

Charbonnier, P., Blanc-Féraud, L., Aubert, G., and Barlaud, M. (1997). Deterministic edge-preserving regularization in computed imaging. *IEEE Transactions on Image Processing*, 6(2):298–311.

Dempster, A., Laird, N., and Rubin, D. (1977). Maximum likelihood from incomplete data via the EM algorithm. *Journal of the Royal Statistical Society, Series B (Methodological)*, 39(1):1–38.

Geman, D. and Reynolds, G. (1992). Constrained restoration and the recovery of discontinuities. *IEEE Transactions on Pattern Analysis and Machine Intelligence*, 14(3):367–383.

Hartley, R. I. and Zisserman, A. (2004). *Multiple View Geometry in Computer Vision*. Cambridge University Press, ISBN: 0521540518, second edition.

Huber, P. J. (1981). *Robust Statistics*. John Wiley and Sons, New York, New York.

Ieng, S.-S., Tarel, J.-P., and Charbonnier, P. (2004). Evaluation of robust fitting based detection. In *Proceedings of European Conference on Computer Vision (ECCV'04)*, pages 341–352, Prague, Czech Republic.

Luenberger, D. G. (1973). *Introduction to linear and nonlinear programming*. Addison Wesley.

Minoux, M. (1986). *Mathematical Programming: Theory and Algorithms*. Chichester: John Wiley and Sons.

Mizera, I. and Müller, C. (1999). Breakdown points and variation exponents of robust m-estimators in linear models. *The Annals of Statistics*, 27(4):1164–1177.

Tarel, J.-P., Ieng, S.-S., and Charbonnier, P. (2002). Using robust estimation algorithms for tracking explicit curves. In *European Conference on Computer Vision (ECCV'02)*, volume 1, pages 492–507, Copenhagen, Danmark.

APPENDIX

We shall first rewrite the value $-e_{MLE}(A)$ for any given $A=(A_j), j=1,\cdots,m$ as the value achieved at the minimum of a convex problem under convex constraints. This is obtained by introducing the auxiliary variables $w_{ij}=(\frac{X_i^tA_j-y_i}{s})^2$. This apparent complication is in fact valuable since it allows us to introduce Lagrange multipliers, and thus to decompose the original problem in simpler problems. The value $-e_{MLE}(A)$ can be seen as the minimum value, w.r.t. $W=(w_{ij})_{1\leq i\leq n,1\leq j\leq m}$, of:

$$E(A,W)=\sum_{i=1}^{i=n} ln(\sum_{j=1}^{j=m} e^{-\frac{1}{2}\phi(w_{ij})})$$

subject to nm constraints $h_{ij}(A,W)=w_{ij}-(\frac{X_i^tA_j-y_i}{s})^2\leq 0$. This is proved by showing that the bound on each w_{ij} is always achieved. Indeed $E(A,W)$ is decreasing w.r.t. each w_{ij}, since its first derivative:

$$\frac{\partial E}{\partial w_{ij}}=-\frac{1}{2}\frac{e^{-\frac{1}{2}\phi(w_{ij})}}{\sum_{k=1}^{k=m} e^{-\frac{1}{2}\phi(w_{ik})}}\phi'(w_{ij})$$

is always negative, due to (H1).

To prove the local convergence of the SMRF algorithm in Sec. 3, we now focus on the minimization of $E(A,W)$ w.r.t. W only, subject to the nm constraints $h_{ij}(A,W)\leq 0$, w.r.t. W, for any A. We now introduce a classical result of convex analysis (Boyd and Vandenberghe, 2004): the function $g(Z)=log(\sum_{j=1}^{j=m} e^{z_j})$ is convex. Due to (H1) and (H2), $-\phi(w)$ is convex and decreasing. Therefore, $E(A,W)$ w.r.t. W is convex as a sum of functions g composed with $-\phi$, see (Boyd and Vandenberghe, 2004). As a consequence, the minimization of $E(A,W)$ w.r.t. W is well-posed because it is a minimization of a convex function subject to convex (linear) constraints. We are thus allowed to apply Kuhn and Tucker's classical theorem (Minoux, 1986): if a solution exists, the minimization of $E(A,W)$ w.r.t. W is equivalent to searching from the unique saddle point of the Lagrange function of the problem:

$$\begin{aligned} L_R(A,W,\Lambda) &= \sum_{i=1}^{i=n} ln(\sum_{j=1}^{j=m} e^{-\frac{1}{2}\phi(w_{ij})}) \\ &\quad +\sum_{i=1}^{i=n}\sum_{j=1}^{m}\frac{1}{2}\lambda_{ij}(w_{ij}-(\frac{X_i^tA_j-y_i}{s})^2) \end{aligned}$$

where $\Lambda=(\lambda_{ij}), 1\leq i\leq n, 1\leq j\leq m$ are Kuhn and Tucker multipliers ($\lambda_{ij}\geq 0$). More formally, we have proved for any A:

$$-e_{MLE}(A)=\min_W \max_\Lambda L_R(A,W,\Lambda) \qquad (11)$$

Notice that the Lagrange function L_R is quadratic w.r.t. A, unlike the original error e_{MLE}. Using the saddle point property, we can change the order of variables W and Λ in (11). We now introduce the *dual function* $\mathcal{E}(A,\Lambda)=\min_W L_R(A,W,\Lambda)$, and rewrite the original problem as the equivalent following problem:

$$\min_A e_{MLE}(A)=\min_{A,\Lambda} -\mathcal{E}(A,\Lambda)$$

The algorithm consists in minimizing $-\mathcal{E}(A,\Lambda)$ w.r.t. A and Λ alternately. $\min_\Lambda -\mathcal{E}(A,\Lambda)$ leads to Kuhn and Tucker's conditions:

$$\lambda_{ij}=\frac{e^{-\frac{1}{2}\phi(w_{ij})}}{\sum_{k=1}^{k=m} e^{-\frac{1}{2}\phi(w_{ik})}}\phi'(w_{ij}) \qquad (12)$$

$$w_{ij}=(\frac{X_i^tA_j-y_i}{s})^2 \qquad (13)$$

and $\min_{A_j} -\mathcal{E}(A,\Lambda)$ leads to:

$$(\sum_{i=1}^{i=n}\lambda_{ij}X_iX_i^t)A_j=\sum_{i=1}^{i=n}\lambda_{ij}y_iX_i,\ 1\leq j\leq m \qquad (14)$$

Using classical results, see e.g. (Minoux, 1986), $-\mathcal{E}(A,\Lambda)$ is proved to be convex w.r.t. Λ. The dual function is clearly quadratic and convex w.r.t. A. As a consequence, this implies that such an algorithm always strictly decreases the dual function if the current point is not a stationary point (i.e a point where the first derivatives are all zero) of the dual function (Luenberger, 1973). The problem of stationary points is easy to solve by checking the positiveness of the Hessian matrix of $\mathcal{E}(A,\Lambda)$. If this matrix is not positive, we disturb the solution so that it converges to a local minimum. This proves that the algorithm is globally convergent, i.e, it converges toward a local minimum of $e_{MLE}(A)$ for all initial A_0's which are neither a maximum nor a saddle point.